[CANCER RESEARCH 63, 3805–3811, July 1, 2003]

Intravascular Metastatic Cancer Cell Homotypic Aggregation at the Sites of Primary Attachment to the Endothelium[1]

Vladislav V. Glinsky,[2] Gennadi V. Glinsky, Olga V. Glinskii, Virginia H. Huxley, James R. Turk, Valeri V. Mossine, Susan L. Deutscher, Kenneth J. Pienta, and Thomas P. Quinn

Departments of Biochemistry [V. V. G., V. V. M., S. L. D., T. P. Q.], Physiology [O. V. G., V. H. H.], and Veterinary Biomedical Sciences [J. R. T., V. H. H.], University of Missouri, Columbia, Missouri 65211; Harry S. Truman Memorial Veterans Hospital [V. V. G., O. V. G., S. L. D.], Columbia, Missouri 65201; Sidney Kimmel Cancer Center and Metastat, Inc. [G. V. G.], San Diego, California 92121; and Departments of Internal Medicine and Urology [K. J. P.], University of Michigan, Ann Arbor, Michigan 48109

ABSTRACT

The two major theories of cancer metastasis, the seed and soil hypothesis and the mechanical trapping theory, view tumor cell adhesion to blood vessel endothelia and cancer cell aggregation as corresponding key components of the metastatic process. Here, we demonstrate *in vitro*, *ex vivo*, and *in vivo* that metastatic breast and prostate carcinoma cells form multicellular homotypic aggregates at the sites of their primary attachment to the endothelium. Our results suggest that metastatic cell heterotypic adhesion to the microvascular endothelium and homotypic aggregation represent two coordinated subsequent steps of the metastatic cascade mediated largely by similar molecular mechanisms, specifically by interactions of tumor-associated Thomsen-Friedenreich glycoantigen with the β-galactoside-binding protein, galectin-3. In addition to inhibiting neoplastic cell adhesion to the endothelium and homotypic aggregation, disrupting this line of intercellular communication using synthetic Thomsen-Friedenreich antigen masking and Thomsen-Friedenreich antigen mimicking compounds greatly affects cancer cell clonogenic survival and growth as well. Thus, β-galactoside-mediated intravascular heterotypic and homotypic tumor cell adhesive interactions at the sites of a primary attachment to the microvascular endothelium could play an important role during early stages of hematogenous cancer metastasis.

INTRODUCTION

Aberrations in cancer cell adhesion play an important role in tumor progression, invasiveness, and metastasis (1, 2). Initially, a decrease in homotypic and heterotypic cancer cell adhesion, caused by the reduced expression of E-cadherins and elevated activity of proteolytic enzymes, including numerous metalloproteinases, promotes their escape from a primary tumor and intravasation (3, 4). During postintravasation stages, however, the increased ability of blood-borne metastatic cells to engage into new heterotypic and homotypic adhesive interactions could be critically important for establishing secondary lesions in distant tissues and organs (5, 6). Two major theories describing cancer metastasis, the seed and soil hypothesis and the mechanical trapping theory, emphasize heterotypic tumor cell adhesion to blood vessel endothelia and homotypic cancer cell aggregation as corresponding key components of the metastatic cascade (reviewed in Ref. 7).

Neoplastic cell heterotypic adhesion to the microvascular endothelium, resulting in tumor cell arrest in the vasculature of a target organ, is an essential early step in hematogenous cancer spread (5). Recent observations, suggesting that only endothelium-attached malignant cells are capable of giving rise to hematogenous cancer metastases, strongly support this idea (8). Moreover, a possible role for tumor-endothelial cell interactions in defining tissue specificity of breast and prostate cancer metastasis was recently revealed (9, 10).

Homotypic tumor cell adhesion (aggregation) leads to the formation of multicellular malignant cell aggregates. Because multicellular clumps could be trapped in small capillaries, the role for homotypic aggregation was postulated within the mechanical trapping theory of cancer metastasis (11). Early pioneering works from the groups of Drs. Isaiah Fidler, Reuben Lotan, Garth Nicolson, and Avraham Raz (12–14), as well as our previous results (6, 15), demonstrated that cancer cells with high metastatic potential exhibit a superior ability to form homotypic aggregates compared with their low metastatic counterparts. In several different types of cancer, the *in vivo* selection of tumor cells for high metastatic potential resulted in a selection of malignant cells exhibiting increased homotypic aggregation properties (6, 12). In addition, cancer cell lines selected *in vitro* for enhanced homotypic aggregation kinetics demonstrated significantly higher *in vivo* experimental metastatic potential than parental cells (14). To date, metastatic cancer cell heterotypic and homotypic adhesion have been largely studied as two independent unrelated processes. Here, we demonstrate in *in vitro*, *ex vivo*, and *in vivo* experiments that these two processes appear to be linked together. Furthermore, it appears that in both breast and prostate cancer, heterotypic and homotypic adhesion mediated largely by similar molecular mechanisms, specifically by interactions between tumor-associated T[3] glycoantigen (3) and galectin family proteins. The results presented in this article suggest that hematogenous cancer metastases could originate from multicellular aggregates formed at the sites of primary tumor cell attachment to the vascular wall. We identify interactions between T antigen and galectin-3 as one of the major pathways for mediating heterotypic and homotypic cancer cell adhesion and promoting metastatic cell clonogenic survival and growth.

MATERIALS AND METHODS

Antibodies, Chemicals, and Reagents. The TIB-166 hybridoma, producing rat monoclonal anti-galectin-3 antibody, was from American Type Culture Collection. T-HSA was from Dextra Laboratories (Reading, United Kingdom). T antigen-binding peptide P-30 (HGRFILPWWYAFSPS) was chemically synthesized using *N*-(9-fluorenyl)methoxycarbonyl-based chemistry. All other chemicals and reagents, unless otherwise specified, were from Sigma (St. Louis, MO).

Cell Lines and Cultures. The MDA-MB-435 human breast carcinoma cell line was provided by Dr. Janet Price (M. D. Anderson Cancer Center, Houston, TX). The DU-145 human prostate carcinoma cells were from American Type Culture Collection (Manassas, VA). The RPMI 1640 supplemented with L-glutamine, 10% FBS, sodium pyruvate, and nonessential amino acids was used for tumor cell lines. Immediately before adhesion experiments, cancer cells were prelabeled for 5 min with 3 μg/ml solution of acridine orange in

Received 12/20/02; accepted 4/23/03.

The costs of publication of this article were defrayed in part by the payment of page charges. This article must therefore be hereby marked *advertisement* in accordance with 18 U.S.C. Section 1734 solely to indicate this fact.

[1] This work was supported, in part, by NIH Grants P20 CA86290-01 (to V. V. G.), 1R43CA72284 and 1RO1CA89827-01 (to G. V. G.), T32 HL07094 (to O. V. G.), R37 HL-42528-13 and PO1 HL52490-06 (to V. H. H.), RO1 HL-36088-16 (to J. R. T.), P50 CA69568 (to K. J. P.), and DOE ER 62027 (to T. P. Q.).

[2] To whom requests for reprints should be addressed, at Department of Biochemistry, University of Missouri, 117 Schweitzer Hall, Columbia, MO 65211. Phone: (573) 814-6000, ext. 3691; Fax: (573) 814-6551; E-mail: glinskiivl@missouri.edu.

[3] The abbreviations used are: T, Thomsen-Friedenreich; HUVEC, human umbilical vein endothelial cells; HBMEC, human bone marrow endothelial cell; HLMVEC, human lung microvascular endothelial cell; FBS, fetal bovine serum; ASF, asialofetuin; T-HSA, T antigen-human serum albumin conjugate; lactulosyl-L-leucine, *N*-(1-deoxy-4-*O*-(β-D-galactopyranos-1-yl)-D-fructofuranos-1-yl)-(S)-2-amino-4-methylpentanoic acid; CCD, charge coupled device.

RPMI 1640, rinsed three times with serum-free RPMI 1640, dissociated from plastic using a nonenzymatic cell dissociation reagent (Sigma), and pipetted to produce a single cell suspension. To remove any remaining cell clumps, tumor cell suspension was filtered through a 20-μm nylon mesh and adjusted to contain 5×10^4 cell/ml. A fresh neoplastic cell suspension was prepared before every injection.

Human bone marrow endothelial cell line HBMEC-60 was provided by Dr. C. Ellen van der Schoot (University of Amsterdam, Amsterdam, the Netherlands). This cell line was developed by immortalization of HBMECs originally isolated from adult human bone marrow using the amphotrophic helper-free retrovirus pLXSN16 E6/E7 (16). The HBMEC-60 cells were shown to maintain their normal phenotype and adhesive properties, specifically the ability to bind hematopoietic progenitor cells (16). The basal Medium 200 (Cascade Biologics, Portland, OR) supplemented with 20% FBS and low-serum growth supplement containing hydrocortisone, human fibroblast growth factor, heparin, and human epidermal growth factor was used for HBMEC-60.

***In Vitro* Parallel Flow Chamber Assay.** The adhesion of MDA-MB-435 and DU-145 cells to HBMECs was studied in an *in vitro* parallel plate laminar flow chamber as follows. HBMEC-60 was grown until 100% confluent in 35-mm tissue culture dishes coated with poly-L-lysine (10 μg/ml) overnight at 4°C. The endothelial cells were exposed to increasing wall shear stress levels in an 100-μm thick parallel plate flow chamber (Glycotech, Rockville, MD) by perfusing warm media (RPMI containing 0.75 mM Ca^{2+} and Mg^{2+} and 0.2% HSA) through a precision syringe infusion/withdrawal pump KDS210 (KD Scientific, New Hope, PA). Next, a single cell suspension of MDA-MB-435 or DU-145 cells (5×10^4 cells/ml) was perfused for a 15-min period. Tumor cell interactions with HBMECs were observed using an inverted phase contrast microscope Diavert (Leitz Wetzlar, Wetzlar, Germany) and video recorded for subsequent offline frame-by-frame analysis.

Perfused Porcine Dura Mater Model. The dura mater corresponding to one hemisphere was collected from 9–12 month-old mature male (for prostate cancer experiments) or female (for breast cancer experiments) Yucatan miniature swine within 15–30 min after animal's sacrifice and immediately placed on ice in a porcine Krebs solution (Krebs physiological salt supplemented with 1.0 mg/ml porcine albumin). The collected dura was dissected to allow for a flattening onto Sylgard-coated 100-mm dish and transferred onto the fluorescent video microscope stage. One of the branches of a *Median Meningeal artery* (typically 300–400 μm inside diameter) was cannulated using a pipette manufactured from 1-mm outer diameter borosilicate glass capillary with a 90-μm opening at the tip.

Dura mater vasculature was perfused at 30 μl/min first with porcine Krebs solution for 20 min, then with 0.3 μg/ml acridine orange solution in RPMI 1640 supplemented with 10% FBS and 1.0 mg/ml porcine albumin for an additional 40 min to visualize the perfused vascular tree. Immediately before injection, the DU-145 or MDA-MB-435 cells, prelabeled for 5 min with 3 μg/ml acridine orange solution in RPMI 1640, were dissociated from plastic and pipetted to produce a single cell suspension.

A single tumor cell suspension (5×10^4 cells/ml) was injected into the system using a chromatography injector with all Teflon-vetted parts and a 250-μl loop. Tumor cell adhesive interactions with dura microvasculature were monitored using a video microscopy system, assembled on the basis of a fixed stage fluorescent microscope Laborlux 8 (Leitz Wetzlar), equipped with a 75-W illuminator and FITC and Rhodamine filter cubes. Video images were acquired with a high sensitivity solid-state CCD video camera (COHU, Inc., San Diego, CA) and recorded at 30 frames/second.

***In Vivo* MDA-MB-435 Breast Carcinoma Cell Adhesion to Mouse Lung Microvasculature.** Six-week-old CB-17/ICR-SCID female mice (Harlan Sprague Dawley) were injected in the tail vein with a single cell suspension of acridine orange-labeled human carcinoma cells (2×10^6). Three h after injection, the animals were euthanized, lungs removed, and examined under a fluorescent microscope Laborlux 8 (Leitz Wetzlar), equipped with a 75-W illuminator and FITC and Rhodamine filter cubes. Video images were acquired with a high sensitivity solid-state CCD video camera (COHU, Inc.) and recorded at 30 frames/second.

Homotypic Aggregation Assay. The effect of various concentrations (0–1.0 mM) of the lactulosyl-L-leucine and lactitol-L-leucine on DU-145 prostate carcinoma cell spontaneous aggregation was assessed using a homotypic aggregation assay as previously described (6, 13).

Clonogenic Survival and Clonogenic Growth. The MDA-MB-435 and DU-145 cells, grown until 50–60% confluent, were harvested using a nonenzymatic cell dissociation reagent as described above and plated at low density in quadruplicate (100 and 200 viable cells/well) in a 24-well culture plate without (control) or in the presence of compounds tested. Only cells with a viability of $\geq$95% were used. Seven days later, the cells were fixed with 1% formaldehyde in PBS, stained with hematoxylin, and colonies of $>$10 cells were scored.

Immunofluorescence and Laser Confocal Scanning Microscopy. The analysis of a galectin-3 cellular distribution was performed exactly as described previously (10, 17, 18). The rat anti-galectin-3 and goat Texas Red-conjugated antirat antibodies were used to visualize galectin-3 by laser scanning confocal microscopy performed on a Bio-Rad MRC 600 confocal system. Z stacks were prepared with 0.5-μm increments and analyzed in orthogonal projections (Y-Z and X-Z sections) using the MetaMorph Imaging System software (Universal Imaging, Hallis, NH). On selected orthogonal plans, to illustrate a gradient of intracellular galectin-3 expression, different colors were assigned to the areas expressing different fluorescence intensities associated with anti-galectin-3 antibody binding (purple, blue, green, yellow, and red from lowest to highest) using a Pseudocolor function of the MetaMorph Imaging System software.

The immunofluorescent analysis of the galectin-3 cell surface expression on live, nonfixed, and nonpermeabilized endothelial or neoplastic cells after a 45-min incubation at 37°C without (control) or with 1 mg/ml (final concentration) bovine fetuin or ASF or 0.5 mg/ml (final concentration) HSA or T-HSA was performed exactly as described previously (10). The computer-assisted morphometric analysis was performed using the MetaMorph Imaging System software.

RESULTS

Although, many important facts regarding tumor-endothelial cell adhesion have been revealed using static adhesion assays, intravascularly they interact under dynamic flow conditions. Under these conditions, physiological shear force dramatically affects the adhesive behavior of both endothelial and neoplastic cells (19). Therefore, we attempted to dissect adhesive mechanisms relevant to cancer metastasis by investigating how metastatic cancer cells interact with endothelia derived from different anatomical sites in flow using parallel flow chamber techniques. Recently, we reported that under conditions of physiological shear force (0.8–4.0 dyn/cm^2) upon adhesion to HLMVEC monolayer, highly metastatic MDA-MB-435, but not nonmetastatic MDA-MB-468, breast carcinoma cells acquired enhanced homotypic aggregation properties. Within minutes of adhesive interactions of a single cell suspension of MDA-MB-435 cells with HLMVEC monolayer, we frequently observed that adherent tumor cells captured other rolling and floating neoplastic cells and initiated a rapid formation of multicellular cancer cell aggregates at the sites of their primary attachment to the endothelia (18). Importantly, this adhesion pattern is not unique to breast carcinoma cell interactions with HLMVECs. Both metastatic breast (MDA-MB-435) and prostate (DU-145) cells exhibit similar adhesion behavior in flow (Fig. 1, *A* and *B*) while interacting with HBMECs representing a tissue most frequently targeted by breast and prostate cancer metastasis. This is an important observation because, although both MDA-MB-435 and DU-145 metastatic human cancer cells also adhere to endothelial cells from the tissues not targeted by tumor metastasis such as HUVECs (9, 10, 17), we previously demonstrated that multiple human prostate carcinoma cell lines, including DU-145 adhere 3–5-fold greater to HBMECs than to HUVECs, aortic endothelial cells, or even HLMVECs (9). We next investigated whether such homotypic cancer cell aggregation occurs intravascularly.

To address these questions, we have used an *ex vivo* experimental system for studying cancer cell adhesive interactions with perfused porcine dura mater microvessels recently developed in our laboratory

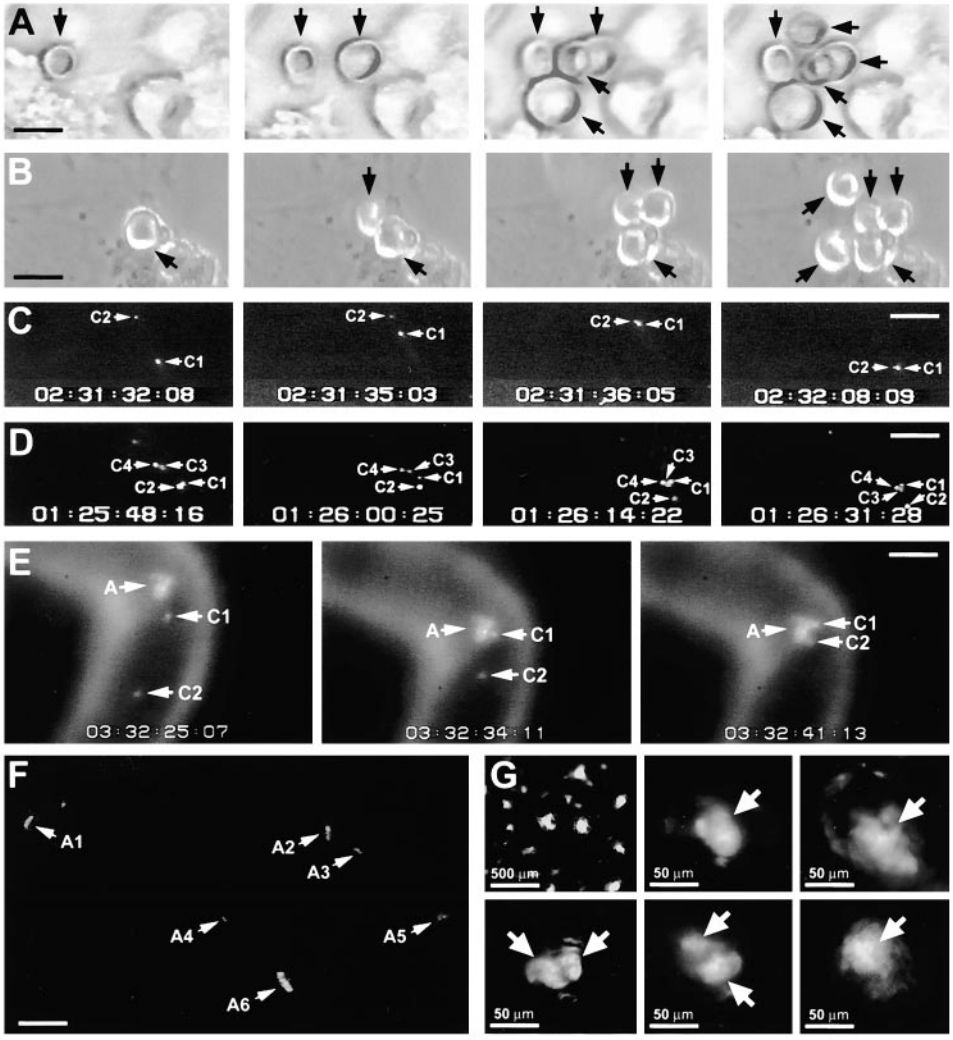

Fig. 1. Multicellular aggregate formation at the site of primary adhesion to the HBMEC monolayer by highly metastatic MDA-MB-435 human breast carcinoma (*A*) and DU-145 human prostate carcinoma (*B*) cells *in vitro* in parallel flow chamber. *C*, intravascular homotypic aggregation of DU-145 human prostate cancer cells *ex vivo* in perfused dura mater microvessels. Rolling (C2) tumor cell approaches stably adhered (C1) cell to form a two-cell aggregate, which remains stably adhered to the vascular wall. *D*, *ex vivo* intravascular homotypic aggregate formation by MDA-MB-435 cells. Rolling (C2) tumor cell interacts temporarily with stably adhered (C1) cell and becomes stably adhered ~30 μm downstream, whereas other two rolling cells (C3 and C4) form stable three-cell aggregate with permanently adhered cell C1. *E*, two rolling DU-145 cells C1 and C2 approach and join a large multicellular aggregate residing in a big arteriole. *F*, multiple DU-145 prostate cancer cell aggregates, *A1–A6* (*arrows*), residing in different vessels within the same observation field. *G*, multiple MDA-MB-435 human breast carcinoma cell aggregates (*arrows*) formed *in vivo* in mouse subpleural precapillary arterioles 3 h after i.v. injection of a single cell suspension. *Scale bars*, 25 μm in *A* and *B*; 100 μm in *C–F*, as indicated in *G*.

(20). Both DU-145 prostate and MDA-MB-435 breast carcinoma cells exhibited *ex vivo* in our intravascular model an adhesion behavior strikingly similar to such of the MDA-MB-435 in parallel flow chamber experiments *in vitro* (Fig. 1, *C–E*). When DU-145 or MDA-MB-435 cells were injected as a single cell suspension into a porcine dura mater microvasculature perfused at the physiological rate, stably adhered carcinoma cells also frequently initiated homotypic aggregation by capturing other circulating tumor cells (Fig. 1, *C* and *D*). In some instances, such homotypic aggregation resulted in a formation of huge multicellular clumps within the vessels far exceeding neoplastic cells in diameter (Fig. 1*E*). These results demonstrate that homotypic cancer cell aggregation at the site of primary attachment to the endothelium occurs when breast and prostate cancer cells interact intravascularly with the endothelia of well-differentiated intact microvessels. Moreover, in perfused dura mater experiments, we often identified multiple homotypic tumor cell aggregates, formed in different microvessels, within the same observation field (Fig. 1*F*), implying that this is not a rare event but rather a common trend. Importantly, highly metastatic MDA-MB-435 breast carcinoma cells exhibited similar adhesion behavior *in vivo*. Injected i.v. as a single cell suspension into SCID mice, blood-borne MDA-MB-435 cells formed multiple intravascular homotypic aggregates stably adhered within mice lung microvessels (Fig. 1*G*).

Both *ex vivo* (Fig. 1, *E* and *F*) and *in vivo* (Fig. 1*G*) homotypic cancer cell aggregates reside frequently in microvessels exceeding significantly the size of the aggregates. This suggests that heterotypic adhesion to the endothelium rather than mechanical trapping is responsible for their arrest in the microcirculation. However, in some instances, it is possible that aggregates may detach and become blood borne once again, in which case one can reasonably envision their additional entrapment in small capillaries. In addition, we cannot completely rule out a multicellular neoplastic cell aggregation resulting from homotypic interactions between two or more floating tumor cells, which could lead, presumably, to mechanical lodging of such aggregates in blood microvessels as well. However, we demonstrate here (Fig. 2) that multiple circulating cancer cells, even while in a very close proximity to each other, can pass freely through a very narrow capillary network without forming multicellular clumps and being trapped (Fig. 2*A*). These same cells do form homotypic aggregates and become permanently lodged when halted by another single cancer cell stably adhered to the microvessel wall (Fig. 2, *B–E*). Once again, in this example, stable heterotypic tumor-endothelial cell adhesion precedes homotypic aggregate formation and permanent neoplastic cell arrest in the microcirculation.

Additional evidence suggests that heterotypic adhesion is not simply a result of mechanical trapping. When heterotypic cancer cell adhesion with endothelia does not take place, tumor cells demonstrate striking ability to avoid mechanical trapping by adjusting their shape and passing through the narrow microvessel sections (Fig. 3). In this particular experiment, prostate cancer cells avoided mechanical en-

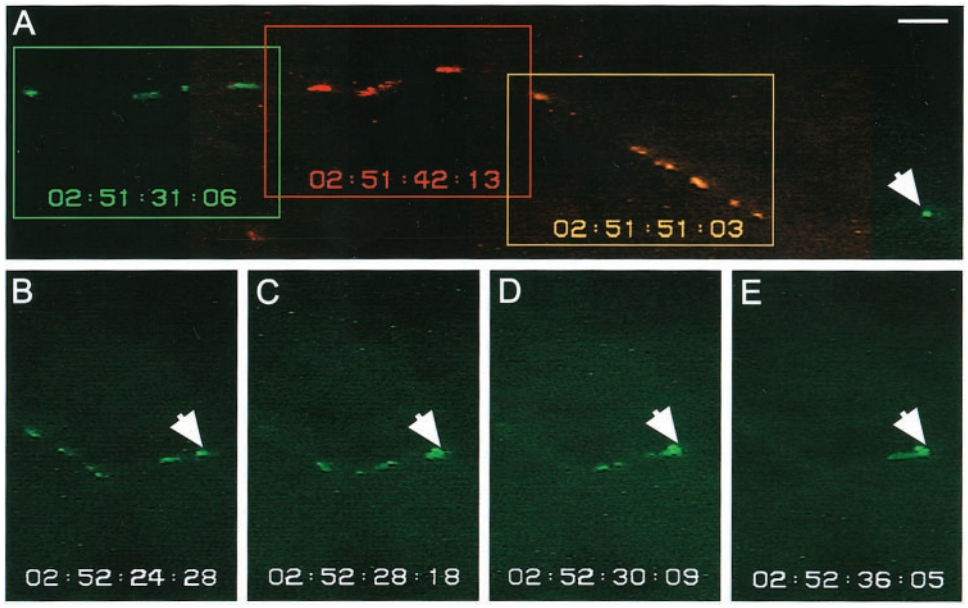

Fig. 2. The group of 12 DU 145 prostate carcinoma cells, lined up in a long narrow capillary, slowly approaches stably adhered neoplastic cell (*arrow*) without interacting with each other or being arrested in circulation. Subsequent frames, illustrating dynamics of tumor cell transition through the microvessel, are represented by *green*, *red*, and *yellow colors*. *B–E*, cancer cells shown in *A* become permanently lodged and form multicellular aggregate when halted by the stably adhered tumor cell. *Scale bar*, 100 μm.

trapment at the site of a microvascular spasm but became permanently attached to the vascular wall ~50 μm downstream of the constricted site in a wide part of the microvessel far exceeding the malignant cell size (Fig. 3). This observation highlights once again the role of heterotypic cancer-endothelial cell adhesion as an essential initial step in circulating metastatic cell permanent arrest within a microvasculature of a target organ.

Collectively, our *in vitro*, *ex vivo*, and *in vivo* results demonstrate that either within relatively large vessels, far exceeding tumor cells in diameter or within narrow capillaries, homotypic tumor cell aggregation is often initiated by preceding heterotypic adhesion between cancer cells and microvascular endothelium. These observations strongly suggest that intravascular heterotypic and homotypic metastatic cell adhesive interactions represent two coordinated subsequent steps of a metastatic cascade.

We next investigated how these processes may be mediated at the molecular level. We previously have reported that heterotypic and homotypic cancer cell adhesion appear to be mediated at least, in part, by similar molecular mechanisms, specifically by interactions between cancer-associated carbohydrate T antigen and β-galactoside-binding galectin family proteins (9, 10, 17, 18). The immunodominant portion of the T antigen, a simple mucin-type core 1 disaccharide Galβ1–3GalNAc, which is masked covalently or structurally on most normal cells, is exposed and immunoreactive on the outer cell surfaces of most human carcinomas and T-cell lymphomas (21, 22). This carbohydrate structure plays an important role in breast and prostate cancer cell adhesion to the endothelium and homotypic aggregation (10, 17, 18, 23–26). Here, we demonstrate that lactulosyl-L-leucine (23, 26), which mimic T antigen (10) but not lactitol-L-leucine (10), is capable of disrupting almost entirely the DU-145 human prostate carcinoma cell homotypic aggregation (Fig. 4*A*). This result indicates that, similarly to breast cancer, prostatic malignant cell homotypic aggregation appears to be largely T antigen mediated.

Of particular significance, in addition to promoting cancer cell homotypic aggregation, this line (T antigen mediated) of intercellular communication is also important in neoplastic cell clonogenic survival (Fig. 4*B*) and clonogenic growth (Fig. 4*C*). In clonogenic survival experiments, we plated breast (MDA-MB-435) and prostate (DU-145) carcinoma cells at the low density (100 or 200 cell/well in 24-well plates) in a presence of various concentration of either T antigen-mimicking lactulosyl-L-leucine (0–1.0 mM) or T antigen-masking P-30 peptide (0–50 μM). Although neither one of these two compounds causes any detectable cytotoxic or growth inhibitory effects in regular monolayer cultures, both lactulosyl-L-leucine (Fig.

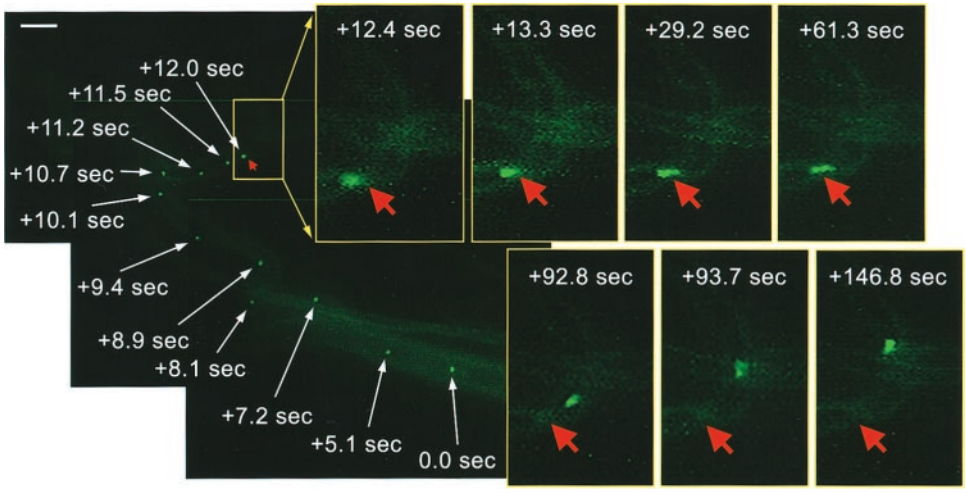

Fig. 3. Rolling tumor cell approaches the site of a microvascular spasm indicated with *red arrow*. By adjusting its shape and passing through the narrow microvessel segment, neoplastic cell avoids mechanical entrapment. However, it becomes permanently adhered ~50 μm downstream in a wide part of a microvessel. *Scale bar*, 50 μm.

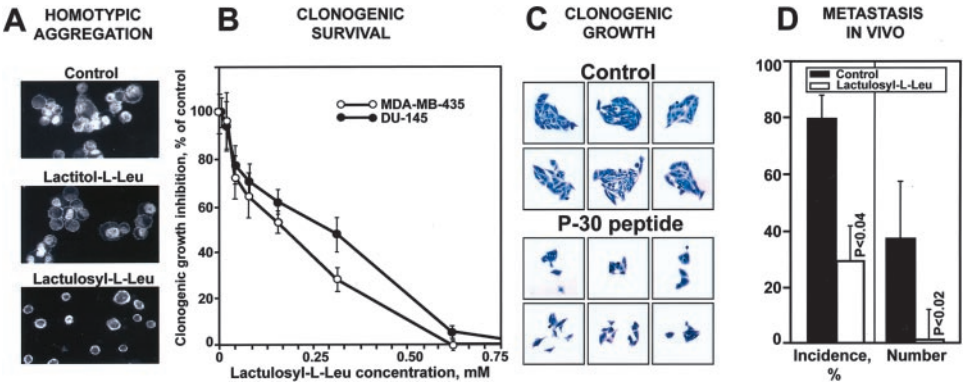

Fig. 4. *A*, the ability of the lactulosyl-L-leucine, but not lactitol-L-leucine (a none-active isomer that differs from lactulosyl-L-leucine only in that the glucose in lactitol is in open, alcohol form), to inhibit homotypic DU-145 prostate cancer cell adhesion. *B*, dose-dependent inhibitory effect of the lactulosyl-L-leucine on MB-435 human breast carcinoma and DU-145 human prostate carcinoma cell clonogenic survival. *C*, the MB-435 human breast carcinoma clones 7 days after plating without (control) or in a presence of 0.1 mg/ml (0.54 μM) T antigen-specific P-30 peptide. *D*, the effect of the lactulosyl-L-leucine on the incidence and number of MB-435 breast cancer metastasis in nude mice experiments.

4*B*) and P-30 (data not shown) inhibited clonogenic survival of breast and prostate cancer cells in a dose-dependent manner. Furthermore, the surviving clones grew at a much slower rate (Fig. 4*C*), suggesting that not only clonogenic survival but also clonogenic growth of cancer cells was affected. These results indicate that in addition to promoting metastatic cell arrest in microcirculation, β-galactoside, specifically T antigen-mediated tumor cell adhesive interactions, could be essential during early stages of metastasis formation by supporting malignant cells clonogenic survival and growth.

This idea is consistent with T antigen interacting with galectin-3. Indeed, lactulosyl-L-leucine, which blocks galectin-3 specifically by mimicking T antigen (10), is capable of inhibiting significantly both incidence and number of spontaneous MDA-MB-435 breast cancer metastasis *in vivo* (Ref. 26 and Fig. 4*D*) in nude mice experiments alone without any cytotoxic drugs. The lactulosyl-L-leucine effects on cancer cell clonogenic survival and growth could be explained at least, in part, through an inhibition by this carbohydrate-amino acid conjugate of β-galactoside-binding lectin galectin-3. Several different groups demonstrated previously the role for this intriguing multifunctional protein in prostate cancer cell adhesion to bone marrow endothelium (9, 10, 17), homotypic cell adhesion (27), protection from apoptosis (28, 29), and MDA-MB-435 breast carcinoma cell anchorage-independent clonogenic growth (30). Recently, we have identified galectin-3 as a binding partner for the T antigen (10, 17). The lactulosyl-L-leucine interacts specifically with galectin-3 by mimicking T antigen (10), thus affecting the functions of this β-galactoside-binding lectin in tumor-endothelial cell heterotypic adhesion, breast and prostate cancer cell homotypic aggregation, and metastatic cell clonogenic survival and growth. Of note, another carbohydrate-based compound also targeting specifically galectin-3, modified citrus pectin developed by the group of Dr. A. Raz, was recently shown to inhibit tumor-endothelial cell adhesion and MDA-MB-435 breast cancer metastasis *in vivo* as well (31).

Consistent with its multiple functions, galectin-3 exhibits multidirectional intracellular trafficking upon various cellular processes. Previously, we reported that during cancer cell adhesion to the endothelia, the endothelium-expressed galectin-3 is clustering toward the sites of heterotypic contacts between endothelial and breast or prostate carcinoma cells (Refs. 10, 17 and Fig. 5, *C–E*, *J*, and *L*, *red arrows*). Recently, Yu *et al.* (32) documented the galectin-3 translocation to the perinuclear membranes in response to various apoptotic stimuli. Here, we demonstrate that in homotypic tumor cell aggregates, galectin-3 is clustering also toward the sites of cancer cell adhesion to each other (Fig. 5*B*, *C*, *F*, *H*, and *K*, *yellow arrows*). In addition and perhaps most intriguing, within minutes of breast and prostate tumor cell interactions with endothelial monolayer, a massive nuclear trafficking of this carbohydrate binding protein occurs in cancer cells (Fig. 5, *C–F*, and *I–L*, *white arrows*).

The galectin-3 clustering toward the sites of heterotypic adhesion on endothelial cells or to the homotypic cell-cell interfaces on tumor cells is consistent with its interactions with T antigen presented on neoplastic cell surfaces (10, 17). Furthermore, the translocation of the galectin-3 to the cell surfaces on both endothelial and cancer cells is also at least, in part, mediated by T antigen (Ref. 10 and Fig. 5, *M* and *N*). We demonstrated previously that T antigen not only acts as the galectin-3 binding partner but also causes rapid galectin-3 mobilization to the endothelial cell outer surfaces (10). Indeed, treating endothelial cells with T antigen conjugated to T-HSA causes >3-fold increase in endothelial cell surface area positively expressing galectin-3 (Fig. 5*M*). Similarly, ASF, a glycoprotein bearing multiple T antigen moieties, but not fetuin, on which T antigen epitopes are covalently masked with sialic (neuraminic) acid, induces rapid increase in galectin-3 surface expression on breast and prostate cancer cells (Fig. 5*N*). In contrast, fetuin was reported by Zhu and Ochieng (33) to induce rapid release of intracellular galectin-3 from tumor cells, suggesting that glycoprotein effect upon cancer cells may depend dramatically on carbohydrate moieties sialylation.

However, what factors cause galectin-3 nuclear translocation remains unknown. Interestingly, this process appears to be specific to neoplastic cell heterotypic adhesion. Galectin-3 nuclear trafficking does not occur when cancer cell interacts with each other (Fig. 5, *B* and *H*). Although, it is also not clear to which of the multiple functions of this intriguing carbohydrate-binding protein this phenomenon is related, it certainly reflects complex signaling pathways triggered by tumor-endothelial cell interactions, which could be critically important in determining the fate of metastatic cancer cells in circulation.

DISCUSSION

Our results suggest that β-galactoside-mediated intravascular heterotypic and homotypic tumor cell adhesive interactions at the sites of a primary attachment to the microvascular endothelium could play an important role in metastatic cancer spread. Interestingly, a similar adhesive behavior was previously reported for selectin-mediated leukocyte adhesion during inflammatory responses (34). Specifically, P-selectin-mediated leukocyte adhesion to the endothelium was shown to trigger a L-selectin-dependent homotypic leukocyte aggregation promoting their cooperative function at the site of inflammation. It appears that similarly heterotypic tumor cell adhesion to the endothelium induces homotypic cancer cell aggregation supporting metastatic cell arrest in microcirculation, clonogenic survival, and growth. However, in leukocytes, this sequence of adhesive events occurs via a coordinated action of P- and L-selectins interacting with their cognate carbohydrate ligands, mostly sialylated Lewis A and Lewis X core 2 oligosaccharides expressed on glycoproteins and

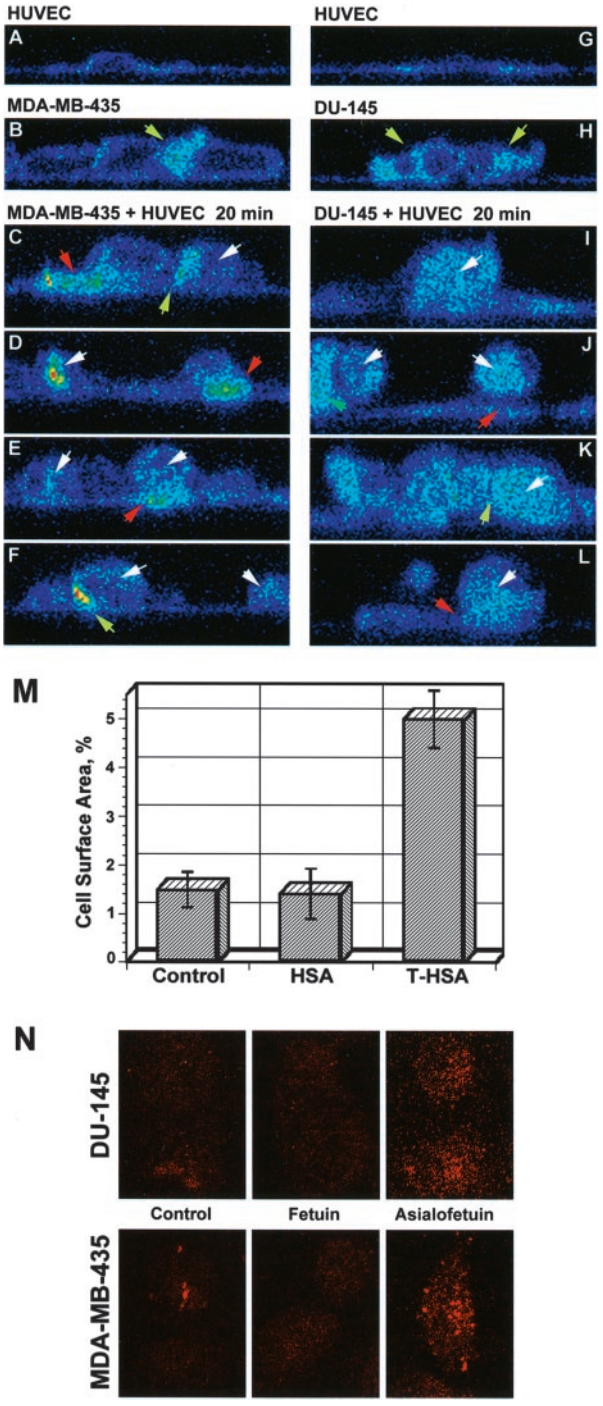

Fig. 5. *A–L*, multidirectional galectin-3 trafficking in tumor and endothelial cells as revealed by laser scanning confocal microscopy. Pseudocolored X-Z and Y-Z orthogonal sections are shown in *A–L*, where different colors represent different concentrations of galectin-3 (*purple*, *blue*, *green*, *yellow*, and *red* from lowest to highest). *A* and *G*, galectin-3 distribution in endothelial cells before interaction with cancer cells. *B* and *H*, orthogonal sections through homotypic aggregates of MDA-MB-435 breast (*B*) and DU-145 prostate (*H*) cancer cells without interacting with endothelia. *C–F* and *I–L*, the galectin-3 on endothelial cells is clustering toward their contacts with cancer cells (*yellow arrows*) and on cancer cells toward the sites of homotypic adhesion (*red arrows*). Note the increase in galectin-3 nuclear localization (*white arrows*) in cancer cells interacting with endothelia (*C–F* and *I–L*) in contrast to neoplastic cells interacting with each other only (*B* and *H*). *M*, changes in endothelial cell surface area percent positively expressing galectin-3 signal after treatment with HSA and T-HSA as revealed by computer-assisted morphometric analysis. Data presented as mean cell surface area percentage ± SD. *N*, T antigen-mediated increase in DU-145 (*top panel*) prostate carcinoma and MDA-MB-435 (*bottom panel*) breast carcinoma cell surface galectin-3 expression. The immunofluorescence experiments were performed on live, nonfixed, and nonpermeabilized cells untreated (control) or treated with fetuin or ASF (1.0 mg/ml final concentration) for 45 min at 37°C.

glycolipids (35, 36). In contrast, our data suggest that in cancer cells, both heterotypic and homotypic adhesion is mediated largely by interactions of the galectin-3 with T antigen core 1 disaccharide desialylated and exposed because of cancer-associated aberrations in neoplastic cell glycosylation. Importantly, this T antigen/galectin-3-mediated sequence of adhesive events appears to be linked to malignant cell metastatic potential because nonmetastatic MDA-MB-468 cells, deficient in both T antigen and galectin-3 expression, do not exhibit similar adhesion behavior (18).

In addition to promoting cancer cell adhesion (10, 17, 18, 26), galectin-3 was directly implicated in malignant cell protection from apoptosis and clonogenic growth (28–30). Thus, the galectin-3 involvement in T antigen-mediated cell-to-cell interactions provides a rationale for explaining the role for this line of intercellular communication in metastatic cell clonogenic survival and growth. Indeed, in several experimental systems, the expression of galectin-3 in cancer cells was associated with increased malignant and metastatic phenotype (37, 38). However, this β-galactoside-binding lectin is not always abundantly expressed in tumor cells. For example, some prostate carcinoma cells such as LNCaP fail to express detectable galectin-3 levels (39, 40). This suggests that other than galectin-3 proteins, perhaps other galectin family members could potentially be involved in neoplastic cell β-galactoside-mediated homotypic interactions.

The signaling pathways triggered by a T antigen engagement most likely depend on which glycoprotein or glycolipid this carbohydrate structure is expressed. For example, the hyaluronan receptor CD44 was identified recently as a major T antigen carrier in colon carcinoma cells (41). The role for CD44 in tumor metastasis, specifically in homing of several different types of cancer to bone marrow as well as in mediating numerous major signaling pathways regulating cell growth, motility, and invasion, is well documented (42–44). The function of this glycoprotein is most studied in a context of its interactions with hyaluronan, a ubiquitous component of the extracellular matrix, which also occurs transiently intracellularly. However, it would be of paramount interest to investigate if CD44-associated signaling pathways in metastatic cells could be activated by galectins through interactions with T antigen. In addition, several other mucin family members implicated in tumor cell adhesion and metastasis such as MUC1, CD146/MUC18/MCAM, or GPI-linked surface mucin CD24 could also be potentially involved in T antigen-mediated adhesion and signaling by expressing this mucin-type disaccharide (45).

In summary, our results suggest that hematogenous cancer metastases could originate from multicellular aggregates formed at the sites of primary tumor cell attachment to the vascular wall resulting at least, in part, from β-galactoside, specifically T antigen-mediated heterotypic and homotypic metastatic cell adhesive interactions. In addition to promoting blood-borne neoplastic cell arrest and retention in a microvasculature of a target organ, these interactions support metastatic cell clonogenic survival and growth, suggesting the involvement of major signaling pathways related to a regulation of cell growth and apoptosis. Unraveling such pathways would greatly enhance our understanding of molecular and cellular mechanisms underpinning tumor metastasis and identify new targets for developing efficient interventive cancer therapies.

REFERENCES

1. Jothy, S., Munro, S. B., LeDuy, L., McClure, D., and Blaschuk, O. W. Adhesion or anti-adhesion in cancer: what matters more? Cancer Metastasis Rev., *14:* 363–376, 1995.
2. Thompson, E. W., and Price, J. T. Mechanisms of tumor invasion and metastasis: emerging targets for therapy. Exp. Opin. Ther. Targets, *6:* 217–233, 2002.

3. Bremnes, R. M., Veve, R., Hirsch, F. R., and Franklin, W. A. The E-cadherin cell-cell adhesion complex and lung cancer invasion, metastasis and prognosis. Lung Cancer, *36:* 115–124, 2002.
4. Curran, S., and Murray, G. I. Matrix metalloproteinases: molecular aspects of their roles in tumor invasion and metastasis. Eur. J. Cancer, *36:* 1621–1630, 2000.
5. Orr, F. W., and Wang, H. H. Tumor cell interactions with the microvasculature: a rate-limiting step in metastasis. Surg. Oncol. Clin. N. Am., *10:* 357–381, 2001.
6. Glinsky, G. V., and Glinsky, V. V. Apoptosis and metastasis: a superior resistance of metastatic cancer cells to programmed cell death. Cancer Lett., *101:* 43–51, 1996.
7. Glinsky, G. V. Anti-adhesion cancer therapy. Cancer Metastasis Rev., *17:* 177–185, 1998.
8. Al-Mehdi, A. B., Tozawa, K., Fisher, A. B., Shientag, L., Lee, A., and Muschel, R. J. Intravascular origin of metastasis from the proliferation of endothelium-attached tumor cells: a new model for metastasis. Nat. Med., *6:* 100–102, 2000.
9. Lehr, J. E., and Pienta, K. J. Preferential adhesion of prostate cancer cells to a human bone marrow endothelial cell line. J. Natl. Cancer Inst. (Bethesda), *90:* 118–123, 1998.
10. Glinsky, V. V., Glinsky, G. V., Rittenhouse-Olsen, K., Huflejt, M. E., Glinskii, O. V., Deutscher, S. L., and Quinn, T. P. The role of Thomsen-Friedenreich antigen in adhesion of human breast and prostate cancer cells to the endothelium. Cancer Res., *61:* 4851–4857, 2001.
11. Fidler, I. J. The relationship of embolic homogeneity, number, size and viability to the incidence of experimental metastasis. Eur. J. Cancer, *9:* 223–227, 1975.
12. Saiki, I., Naito, S., Yoneda, J., Azuma, I., Price, J. E., and Fidler, I. J. Characterization of the invasive and metastatic phenotype in human renal cell carcinoma. Clin. Exp. Metastasis, *9:* 551–566, 1991.
13. Meromsky, L., Lotan, R., and Raz, A. Implications of endogenous tumor cell surface lectins as mediators of cellular interactions and lung colonization. Cancer Res., *46:* 5270–5275, 1986.
14. Updyke, T. V., and Nicolson, G. L. Malignant melanoma cell lines selected *in vitro* for increased homotypic adhesion properties have increased experimental metastatic potential. Clin. Exp. Metastasis, *4:* 273–284, 1986.
15. Glinsky, G. V., Glinsky, V. V., Ivanova, A. B., and Hueser, C. N. Apoptosis and metastasis: increased apoptosis resistance of metastatic cancer cells is associated with the profound deficiency of apoptosis execution mechanisms. Cancer Lett., *115:* 185–193, 1997.
16. Rood, P. M. L., Calafat, J., Von dem Borne, A. E. G. K., Gerritsen, W. R., and van der Schoot, C. E. Immortalisation of human bone marrow endothelial cells: characterization of new cell lines. Eur. J. Clin. Investig., *30:* 618–629, 2000.
17. Glinsky, V. V., Huflejt, M. E., Glinsky, G. V., Deutscher, S. L., and Quinn, T. P. Effects of Thomsen-Friedenreich antigen-specific peptide P-30 on β-galactoside-mediated homotypic aggregation and adhesion to the endothelium of MDA-MB-435 human breast carcinoma cells. Cancer Res., *60:* 2584–2588, 2000.
18. Khaldoyanidi, S. K., Glinsky, V. V., Sikora, L., Glinskii, A. B., Mossine, V. V., Quinn, T. P., Glinsky, G. V., and Sriramarao, P. MDA-MB-435 human breast carcinoma cell homo- and heterotypic adhesion under flow conditions is mediated in part by Thomsen-Friedenreich antigen-galectin-3 interactions. J. Biol. Chem., *278:* 4127–4134, 2003.
19. Haier, J., and Nicolson, G. L. Tumor cell adhesion under hydrodynamic conditions of fluid flow. APMIS, *109:* 241–262, 2001.
20. Glinskii, O. V., Huxley, V. H., Turk, J. R., Deutscher, S. L., Quinn, T. P., Pienta, K. J., and Glinsky, V. V. Continuous real-time *ex vivo* epifluorescent video microscopy for studying cancer cell interactions with dura mater microvasculature. Clin. Exp. Metastasis, in press, 2003.
21. Springer, G. F. T and Tn, general carcinoma autoantigens. Science (Wash. DC), *224:* 1198–1206, 1984.
22. Springer, G. F., Desai, P. R., Ghazizadeh, M., and Tegtmeyer, H. T/Tn pancarcinoma autoantigens: fundamental, diagnostic, and prognostic aspects. Cancer Detect. Prev., *19:* 173–182, 1995.
23. Glinsky, G. V., Mossine, V. V., Price, J. E., Bielenberg, D., Glinsky, V. V., Ananthaswamy, H. N., and Feather, M. S. Inhibition of colony formation in agarose of metastatic breast carcinoma and melanoma cells by synthetic glycoamine analogs. Clin. Exp. Metastasis, *14:* 253–267, 1996.
24. Peletskaya, E. N., Glinsky, V. V., Glinsky, G. V., Deutscher, S. L., and Quinn, T. P. Characterization of peptides that bind the tumor-associated Thomsen-Friedenreich antigen selected from bacteriophage display libraries. J. Mol. Biol., *270:* 374–384, 1997.
25. Rittenhouse-Diakun, K., Xia, Z., Pickhardt, D., Morey, S., Baek, M-G., and Roy, R. Development and characterization of monoclonal antibody to T-antigen: (Galβ1–3GalNAc-α-O). Hybridoma, *17:* 165–173, 1998.
26. Glinsky, G. V., Price, J. E., Glinsky, V. V., Mossine, V. V., Kiriakova, G., and Metcalf, J. B. Inhibition of human breast cancer metastasis in nude mice by synthetic glycoamines. Cancer Res., *56:* 5319–5324, 1996.
27. Inohara, H., and Raz, A. Functional evidence that cell surface galectin-3 mediates homotypic cell adhesion. Cancer Res., *55:* 3267–3271, 1995.
28. Akahani, S., Nangia-Makker, P., Inohara, H., Kim, H-R. C., and Raz, A. Galectin-3: a novel antiapoptotic molecule with a functional BH1 (NWGR) domain of Bcl-2 family. Cancer Res., *57:* 5272–5276, 1997.
29. Kim, H-R. C., Lin, H-M., Biliran, H., and Raz, A. Cell cycle arrest and inhibition of anoikis by galectin-3 in human breast epithelial cells. Cancer Res., *59:* 4148–4154, 1999.
30. Honjo, Y., Nangia-Makker, P., Inohara, H., and Raz, A. Down-regulation of galectin-3 suppresses tumorigenicity of human breast carcinoma cells. Clin. Cancer Res., *7:* 661–668, 2001.
31. Nangia-Makker, P., Hogan, V., Honjo, Y., Baccarini, S., Tait, L., Bresalier, R., and Raz, A. Inhibition of human cancer cell growth and metastasis in nude mice by oral intake of modifie citrus pectin. J. Natl. Cancer Inst. (Bethesda), *94:* 1854–1862, 2002.
32. Yu, F., Finley, R. L., Raz, A., and Kim, H-R. C. Galectin-3 translocates to the perinuclear membranes and inhibits cytochrome *c* release from the mitochondria. J. Biol. Chem., *277:* 15819–15827, 2002.
33. Zhu, W-Q., and Ochieng, J. Rapid release of intracellular galectin-3 from breast carcinoma cells by fetuin. Cancer Res., *61:* 1869–1873, 2001.
34. McEver, R. P. Selectin-carbohydrate interactions during inflammation and metastasis. Glycoconj. J., *14:* 585–591, 1997.
35. Butcher, E. C. Leukocyte-endothelial cell recognition: three (or more) steps to specificity and diversity. Cell, *67:* 1033–1036, 1991.
36. Lawrence, M. B., and Springer, T. A. Leukocytes roll on a selectin at physiologic flow rates: distinction from and prerequisite for adhesion through integrins. Cell, *65:* 859–873, 1991.
37. Nangia-Makker, P., Sarvis, R., Visscher, D. W., Baily-Penrod, J., Raz, A., and Sarkar, F. H. Galectin-3 and L1 retrotransposons in human breast carcinomas. Cancer Res. Treat., *49:* 171–183, 1998.
38. Nangia-Makker, P., Thompson, E., Hogan, C., Ochieng, J., and Raz, A. Induction of tumorigenicity by galectin-3 in a non-tumorigenic human breast carcinoma cell line. Int. J. Oncol., *7:* 1079–1087, 1995.
39. Ellerhorst, J., Nguyen, T., Cooper, D. N. W., Lotan, D., and Lotan, R. Differential expression of endogenous galectin-1 and galectin-3 in human prostate cancer cell lines and effects of overexpressing galectin-1 on cell phenotype. Int. J. Oncol., *14:* 217–224, 1999.
40. Pacis, R. A., Pilat, M. J., Pienta, K. J., Wojno, K., Raz, A., Hogan, V., and Cooper, C. R. Decreased galectin-3 expression in prostate cancer. Prostate, *44:* 118–123, 2000.
41. Singh, R., Campbell, B. J., Yu, L. G., Fernig, D. G., Milton, J. D., Goodlad, R. A., FitzGerald, A. J., and Rhodes, J. M. Cell surface-expressed Thomsen-Friedenreich antigen in colon cancer is predominantly carried on high molecular weight splice variants of CD44. Glycobiology, *11:* 587–592, 2001.
42. Van Driel, M., Gunthert, U., Van Kessel, A. C., Joling, P., Stauder, R., Lokhorst, H. M., and Bloem, A. C. CD44 variant isoforms are involved in plasma cell adhesion to bone marrow stromal cells. Leukemia (Baltimore), *16:* 135–143, 2002.
43. Stapleton, G., Malliri, A., and Ozanne, B. W. Down-regulated AP-1 activity is associated with inhibition of protein-kinase-c-dependent CD44 and ezrin localization and up-regulation of PKC θ in A431 cells. J. Cell Sci., *115:* 2713–2724, 2002.
44. Entwistle, J., Hall, C. L., and Turley, E. A. HA receptors: regulators of signaling to the cytoskeleton. J. Cell. Biochem., *61:* 569–577, 1996.
45. Fonseca, I., Costa Rosa, J., Felix, A., Therkildsen, M. H., and Soares, J. Simple mucin-type carbohydrate antigens (T, Tn and sialosyl-Tn) in mucoepidermoid carcinoma of the salivary glands. Histopathol. (Oxf.), *25:* 537–543, 1994.